International Journal of Environmental Science and Bioengineering
ISSN 2476-4582

Determination of pollution rate in wetland using hydraulic model

Majid Homami[1], Hamid Goshtasb[2*] Behzad Rayegani[2] Javad Ramezani[3]

[1] Ph.D., College of Environment, Karaj- Iran. Email: Homami434@yahoo.com
[2*] Associated Professor, Collage of Environment, Karaj, Iran. Email: meigooni1959@gmail.com; bhz.ray@gmail.com
[3] Assistant Professor, Collage of Environment, Karaj, Iran. Email: jramezani@gmail.com

How to cite this article Homami M. Goshtasb H. Rayegani B. Ramezani J. Saljooghi H. (2019), Determination of Pollution Rate in Wetland Using Hydraulic Model. IJESB 12 (2019) 15-34

Abstract

This article discusses possibility of preparation and prediction of zoning map for the seasons and changes of spatio-temporal distribution of water quality parameters including nutrients using 2D equations of shallow water and their numerical solution and the technique to use the best interpolation method. Based on the research, the velocity of water hydraulic flow can be determined and their impacts on water quality parameters can be studied. The idea of using the 2D flow correction analysis in wetlands using 1D (laboratory data) accurate values is other major results of the research that leads to reduction of fluctuation in results and achieving better convergence in solving the obtained equations. In addition to the comparison of the modeling results and valid results, correlation coefficient and MAE are used for model verification. An appropriate compatibility is observed among the results, as there is a 6-7% correlation among the study parameters. The results obtained from simulation the numerical model and the author-developed software prove that the average annual concentration of nitrate and phosphate in Anzali wetland in 2030 will respectively be about (10.7%) and (15.2%) higher than the present values and the average relative DO will decrease about (14.8%).

Submitted June 2018
Accepted February 2019
Published June 2019
Corresponding author Majid Homami
Academic editor Eskandar Omidinia

Additional Information and Declarations can be found on End of article.

Subjects: Pollution, Environmental engineering, Water resources.
Keywords: wetland, haydraulic mode, pollution rate

INTRODUCTION

Wetlands, as unique, rich, and fertile ecosystems, are among the most productive and valuable natural environments in the world , the most vital factors that preserve waterways and provide human food (Burton and Tiner, 2009). They are called "nature kidneys" (Mitsch and Gosselink, 2007). The ecosystems have natural beauty as well as considerable environmental, social, and economic benefits, because the great functions and benefits of wetlands have made them irreplaceable. Despite the major advances and appropriate studies and research in recent decades on water resources, wetlands are still among the world's most threatened ecosystems including continued drying, addition of contaminants, and excessive use of their sources (Majnonian, 2003).

Anzali International Wetland is one of the most valuable water resources. It is highly considered due to its specific ecological, economic, social conditions, and variety of plant species and aquatic animals. The increase in various urban, industrial, and agricultural activities around Anzali Wetland over the past two decades has flown abundant amount of different pollutants including nitrogen and phosphorus into the wetland, intensified eutrophication, and increased total dissolved solid (TDS) changes. If the current situation persists, the wetland will be destroyed much sooner than its natural destiny (Zebardast and Jafari, 2012). High concentration of nitrogen and phosphorous, which are of major parameters of water quality assessment and consequently the excessive growth of the creatures formed by them such as the considerable growth of the algae and photosynthetic bacteria most of which have caused destructive disorders in balancing organisms and water quality of natural ecosystems like wetlands that are highly sensitive and vulnerable, have made numerous studies carry out by researchers all over the world in this field (Mirbagheri et al., 1981; 1988; 2008; 2010; 2012; 2016a, b; Haji et al., 2013; Shoaei et al., 2018; Biglarijoo et al., 2017).

since it is very costly and sometimes impossible to measure pollution parameters in the whole wetland area in the form of taking specimens is , this research attempted to model spatio-temporal changes and to prepare the zoning map of nutrients and DO contents across Anzali Wetland using assorted spatial interpolation methods and selecting an optimal method. The developed software by the author was used to study the dynamic behavior of water flow and 2D equations of the hydraulic flow of direction and velocity of water flow in the concentration of each nutrient parameter changes [flow dynamics may impact nutrient movement into water, and may be influenced by water level fluctuations, and time (Miller et al., 2017)] and to predict the existing and future quality parameters in the wetland. The research also aims at preparing a numerical model to reduce examination time and evaluate all parameters.

MATERIAL AND METHOD

Predicting the changes in different pollution in a shallow water environment requires calculation of the velocity field (Zerrati et al., 2001).

Governing equations and Numerical solution method

The 2D flow governing equations, which were used for predicting the concentration of the qualitative parameters of shallow water, include convection-diffusion equation (Equation 1) and continuity equation (Equation 2) as follows (Muhammetoglu and Soyupak, 2000).

$$\frac{\partial c}{\partial t} = -\left(u\frac{\partial c}{\partial x} + v\frac{\partial c}{\partial y}\right) + \frac{\partial}{\partial x}\left(D_x\frac{\partial c}{\partial x}\right) + \frac{\partial}{\partial y}\left(D_y\frac{\partial c}{\partial y}\right) \tag{1}$$

$$\frac{\partial c}{\partial t} + \frac{\partial (uc)}{\partial x} + \frac{\partial (vc)}{\partial y} = 0 \tag{2}$$

In these equations, c is concentration of qualitative components (mg/lit), u is the velocity factor along x axis. v is velocity component along y axis, h is depth of water (meter), t is time (day), D_x and D_y are the impact factors in longitudinal and lateral axes (in m/day).

The finite-volume and fractional step methods were used in this research for discontinuing and solving the governing equations.

Solving the displacement equations

The displacement equations in the 2D space is shown in relation (2). The control volume used in the present study is a quadrant created by the perpendicular bisectors of corners. Considering figure 1, if a perpendicular plane passes on jj_1 line, a two-dimensional space similar to one dimensional will be created.

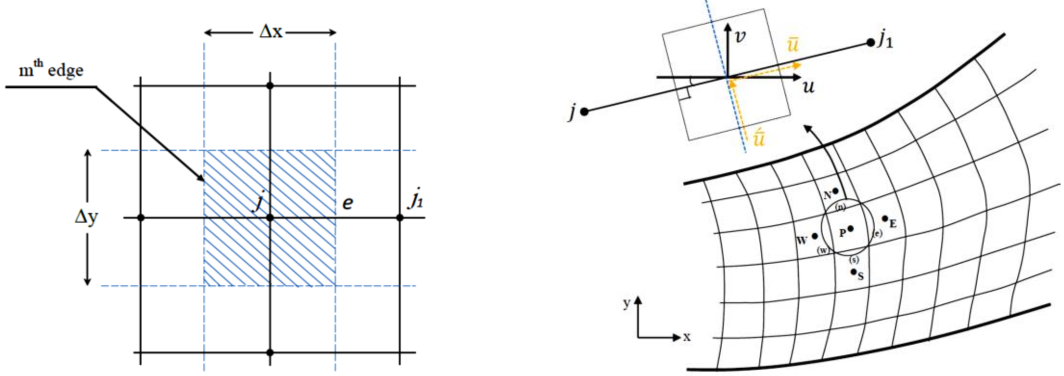

Figure 1. Control volume around point *j* consisting of the cross section of perpendicular bisectors of the sides.

Therefore, for each side line, the two quantity of velocity and concentration ($\bar{u},\bar{c}$) should be calculated in border; we will have:

$$u=\frac{u_j+u_{j_1}}{2} \quad , \quad Sin\theta=\frac{x_{j_1}+x_j}{L_{jj_1}} \tag{3}$$

$$v=\frac{v_j+v_{j_1}}{2} \quad , \quad Cos\theta=\frac{y_{j_1}+y_j}{L_{jj_1}} \tag{4}$$

$$\bar{u}=u\times Cos\theta+v\times Sin\theta \tag{5}$$

$$\bar{u}'=v\times Cos\theta-u\times Sin\theta \tag{6}$$

where L_{jj1} : Length of edge wall jj_1 ,$\bar{u}$: Velocity alongside the edge wall of jj_1 (m/s), $\bar{u}$ ': Velocity alongside perpendicular line on jj_1 side edge (m/s).

$$\bar{c}=\frac{\left[\left(c_j+\frac{\Delta x}{2}S_j\right)+\left(c_j+\left(\frac{\Delta x}{2}-u\Delta t\right)S_j\right)\right]}{2} \quad , \quad S_j=\frac{C_{j+1}-C_{j-1}}{2\Delta x} \tag{7}$$

After determining the amounts of $\bar{u}$ and $\bar{c}$, the transient flux through border is calculated from the following equations (Mohammadzadeh et al., 2005):

$$Flux=\bar{u}.\bar{c}.\Delta s \tag{8}$$

where Δs is the border length.The flux calculated from the node is the first subtracted and then added to the end node. The mentioned operations are carried out for all the edge walls. Ultimately, using equation (9), the amount of c_j^{n+1} was determined.

$$c_j^{n+1}=c_j^n+\Delta t\frac{\sum FluxAdv(j)}{area(j)} \tag{9}$$

In this relation, *Σ Flux Adv (j)* is the algebraic fluxes that enter and exit node j from the control volume borders around it and, *area (j)* is the area of control volume around node *j*.

Solving the dispersion equation

The dispersion equation in two-dimensional space is in form of equation (10).

$$\frac{\partial c}{\partial t}-\frac{\partial}{\partial x}\left(D_x\frac{\partial c}{\partial x}\right)-\frac{\partial}{\partial y}\left(D_y\frac{\partial c}{\partial y}\right)=0 \tag{10}$$

According to figure 2, the flux from dispersion that passes through A_1A_2 borders is calculated in equation (11).

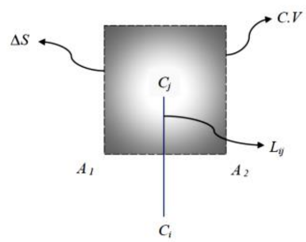

Figure 2. Parameters related to determining dispersion flux.

$$Flux=-D_n\frac{\partial c}{\partial l}\Delta S=-D_n\frac{c_j-c_i}{L}\Delta S \tag{11}$$

In the above equation, D_n is the dispersion factor along side edge *ij*. Other parameters are also defined.

Like the displacement stages, by using relation (12), the amount of c_j^{n+1} is determined.

$$c_j^{n+1}=c_j^n+\Delta t\frac{\sum FluxDiff\,(j)}{area(j)} \tag{12}$$

Solving the two-dimensional equations of shallow waters

If the two-dimensional equations of shallow waters (equation 1) is integrated in control volume and the Gauss divergence theorem is used for converting surface integral to line in the transport and dispersion (diffusion) terms, equation (13) will be obtained as follows:

$$\frac{\partial}{\partial t}\int_{\Omega}Cd\Omega+\oint H.\vec{n}dS=0 \tag{13}$$

where $\vec{n}$ is the perpendicular vector on the side of finite volume, Ω is the area of two-dimensional control volume (m²) and *S* is in its environment (m), *H* is the transient flux of parameter *C* from each aspects of finite volume, including the two terms of transport and dispersion and is written in form of equation (14).

$$H=(F^C+F^D)\vec{\imath}+(G^C+G^D)\vec{\jmath} \tag{14}$$

In this relation (D_x=D_y=D):

$$F^C=uc \qquad , \qquad G^C=vc \tag{15}$$

$$F^D=-D\frac{\partial c}{\partial x} \tag{16}$$

$$G^D = -D\frac{\partial c}{\partial y} \tag{17}$$

By putting the above-mentioned equations in equation (13) and considering the fact that u and v are Cartesian velocities, and by attention to the point that $d\vec{S} = dy\vec{i} - dx\vec{j}$, equation (18) is obtained as follows:

$$\frac{\partial}{\partial t}\int_{\Omega} Cd\Omega + \oint_{S}(Fdy - Gdx) = 0 \tag{18}$$

where,

$$F = F^C + F^D \qquad , \qquad G = G^C + G^D \tag{19}$$

When the values of F and G are specified in the network edges, the environmental integral which is written in equation (18) is calculated as follows:

$$\oint_{S}(Fdy - Gdx) \cong \sum_{e=1}^{N_i}(F_e\Delta y_e - G_e\Delta x_e) \tag{20}$$

where index e is the number of edge walls and N_i is the total number of edge walls in control volume. In addition, the transient flux from each edge wall and C_j^{n+1} is calculated from following equations:

$$Flux_e = F_e\left(y_{j_1} - y_j\right) - G_e\left(x_{j_1} - x_j\right) \tag{21}$$

$$C_j^{n+1} = C_j^n - \left(Flux^C + Flux^D\right)\frac{\Delta t}{A_j} \tag{22}$$

where Aj is the area of control volume, Δt is the time step, $Flux^C$ and $Flux^D$ are the parts related to the flux transient transport and dispersion terms. To use relation (22), the transport and dispersion terms on each edge walls must be calculated as follows:

$$F_e^C = \frac{1}{2}\left(F_j^c + F_{j_1}^c\right) \qquad , \qquad G_e^C = \frac{1}{2}\left(G_j^c + G_{j_1}^c\right) \tag{23}$$

Therefore,

$$Flux^c = \frac{1}{2}\sum_{e=1}^{N_i}\left[\left(F_j^c + F_{j_1}^c\right)\left(y_{j_1} - y_j\right) - \left(G_j^c + G_{j_1}^c\right)\left(x_{j_1} - x_i\right)\right] \tag{24}$$

In terms of dispersion:

$$\left.\frac{\partial c}{\partial x}\right|_j = \frac{1}{A_j}\int_{\Omega}\frac{\partial c}{\partial x}dxdy = \frac{1}{A_j}\oint_{S} cdy \tag{25}$$

Where,

$$A_j = \int_{\Omega} dxdy = \oint_{S} xdy = -\oint_{S} ydx \tag{26}$$

Similarly, for derivative in direction y:

$$\frac{\partial c}{\partial y}\Big|_j = \frac{1}{A_j}\int_{\Omega}\frac{\partial c}{\partial y}dydx = -\frac{1}{A_j}\oint_S cdx \tag{27}$$

When the average of values C on the nodes at both tops of each edge walls are considered as the C value of that edge wall, the equations (25) and (27) could be written in a numerical form as follows:

$$\frac{\partial C}{\partial x}\Big|_j = \frac{1}{A_j}\sum_{e=1}^{N_i}(C\Delta y) = \frac{1}{2A_j}\sum_{e=1}^{N_i}\left[\left(C_j + C_{j_1}\right)\left(y_{j_1} - y_j\right)\right] \tag{28}$$

$$\frac{\partial C}{\partial x}\Bigg|_j = \frac{1}{A_j}\sum_{e=1}^{N_i}(C\Delta x) = \frac{1}{2A_j}\sum_{e=1}^{N_i}\left[\left(C_j + C_{j_1}\right)\left(x_{j_1} - x_j\right)\right] \tag{29}$$

By using the above values and equations (16) and (17), the values of F^D and G^D are calculated in all nodes (Sabbagh-Yazdi et al., 2008). Therefore:

$$Flux^D = \frac{1}{2}\sum_{e=1}^{N_i}\left[\left(F_j^D + F_{j_1}^D\right)\left(y_{j_1} - y_j\right) - \left(G_j^D + G_{j_1}^D\right)\left(x_{j_1} - x_j\right)\right] \tag{30}$$

The Study Area

Anzali International Wetland covers an area of approximately 193 km^2 in north of Iran and southwest of Caspian Sea in Bandar Anzali in Gilan Province. It is located at the latitude 37° 23' to 37° 26' N and longitude 49° 24' to 49° 27' E with the average depth of 2.5-3 m (JICA, 2012). In 1975, the wetland was registered in *Ramsar Convention International Wetlands* (Jones et al., 2008). In addition to its valuable water reserves , historical and tourist attractions, it is highly important due to its location on the route to Europe. Figure 3 shows the location of the study area .

Figure 3. Location, geometrical conditions, and distribution of sampling points in the study area.

Preparation of Zoning Maps

In addition to the 2D equations of hydraulic flow behavior, this research used five Kriging interpolation methods (Relations 31 and 32), inverse distance to power method (Relation 33), polynomial regression method (Relations 34 and 35), and local polynomial (Johnston et al., 2001), and spline method.

$$Z_X^* = \sum_{i=1}^{n} \lambda_i Z_{xi} \tag{31}$$

$$\gamma(h)=\frac{1}{2n(h)}\sum_{i=1}^{n}\left[Z(xi)-Z(xi+h)\right]^{2} \tag{32}$$

where Z_x^* is the estimated value of the variable, and λ_i is the weight related to the variable i^{th}, *n* is number of observations, *γ(h)* is the change of power for the pairs of points with the *h* distance between them, *Z(xi)* is the observed value of variable i^{th}, and *Z(xi +h)*is the observed value of the variable at the distance of *h* from *xi* (Forsythe et al., 2010).

$$W_i=\frac{D_i^{-m}}{\sum_{i=1}^{n} D_i^{-m}} \tag{33}$$

where *Wi* is the weight of the point i^{th}, Di is the distance between the i^{th} specimen point and the unknown point, *m* is the weighting power, and *n* is the number of vicinity points (Hasanipak, 2013).

$$Z=a+bx+cy+dxy+ex^2+fy^2+gx^3+hx^2y+ixy^2+jy^3+\ldots+kx^n+\ldots+ly^n \tag{34}$$

$$\frac{\ln a-\ln b}{\ln t_1-\ln t_2}=\frac{\ln b-\ln x}{\ln t_2-\ln(t_2+t)} \tag{35}$$

where *Z* is the estimated value or the variable, *a* and *b* are the known values obtained from measurements, and t_1 is the elapsed time related to *a*, and t2is the current time of *b*. The value of variable *x* is related to future time of *t*, i.e. (t_2+t) (Viera, 1983). All the interpolation and extrapolation calculations were made in *surfer 9* and *Code Blocks*. The developed software by the author is written in C^{++} in 3740 lines and the mean of laboratory measurements were used in it, which are mainly used for predicting concentration of nutrients in the coming decades. In addition, prior to geostatistical analysis, some common statistical tests like normalization were performed on the data.

Monthly spatial distribution maps for nutrient concentration were created by applying each of the above mentioned interpolation methods on the monthly (NO_3-N) and (PO_4^{-3}) of Anzali Wetland data. The Cross-validation method was used for studying the error of each method and selecting an optimal method for each study parameter. In this method, at each stage one observation point is removed and that point is estimated using the other points. After repeating this procedure for all the observation points, the number of estimates will be equal to one of the observation points. The observational and estimated values are compared and, the best method can be selected using different assessment criteria. RMSE (Relation 36) is one of the assessment criteria that can be used and it was used to compare interpolation methods (Kazemi and Hosseini, 2011).

$$\mathrm{RMSE}=\sqrt{\frac{1}{n}\sum_{i=1}^{n}(Z^*(x_i)-Z(x_i))^2} \tag{36}$$

The closer the value is to zero, the less error a method will have. Therefore, the optimal spatial interpolation method will be obtained for estimating the monthly nitrate and phosphate contents across the wetland by comparing the RMSE achieved by any method for the data of each month. It should be noted that the appropriate interpolation method to estimate a variable depends on the type of variables and regional factors effecting it and the selected method of a region cannot be generalized to other regions. The monthly wetland nitrate and phosphate contents zoning map was prepared after calculating RMSE values and selecting the optimal method. The spatial distribution map for nitrate and phosphate contents in spring, summer, autumn, and winter was prepared by combining the monthly maps and using the monthly spatial distribution of (NO_3-N) and (PO_4^{-3}) contents map. Finally, by comparing the seasonal maps, the temporal changes of (NO_3-N) and (PO_4^{-3}) were assessed at a seasonal time scale.

Wetland Quality Parameters Simulation

After studying the available data and the data of measurement stations, ten stations were selected along the wetland between upstream Bandar Anzali Bridge and the channel connecting Anzali Wetland to the Persian Sea in the middle of the city in an approximate area of 6 kilometers. Simulation was performed in 1D and 2D modes of unsteady flow and entrance of pollutants to wetland water flow (Note that 2D models, which are more accurate than the 3D models in longitudinal and vertical directions in shallow water like wetlands, may control numerical dispersion better than 3D models). Therefore, the 2D computation model is cheaper than 3D models and may provide more accurate simulation at longer time scales (Dorostkar et al., 2005). For this reason, 2D model was used in this research. Factors of nutrients (nitrate and phosphate) and DO were simulated. To simulate the numerical solution network design , the considered rectangular block and system of flows are similar to figure 4.

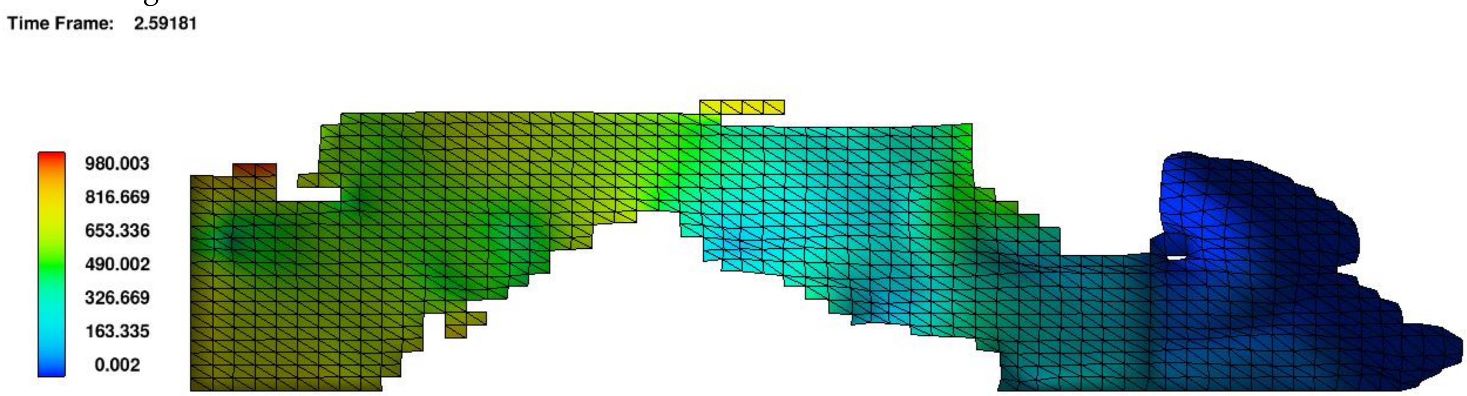

Figure 4. Number of elements and the geometry of shallow waterbed (River and Wetland) in the study area.

This block consists of 10800 cells with 80 m long, 20 m wide and 3 m deep.

The software or FLOW-3D mathematical model was used for 2D simulation. As compared with other similar engineering software such as FLUENT, QUAL2KW, HSPF, AGNPS, CORMIX, SLAMM, ANSYS MIKE, WASP, QUAL2E and MIKE and WASP families have been appropriate on water quality simulation (Bottino et al., 2011; Aliverdi and eslami, 2014; Mohamadi Golafshani et al., 2012; Mirbagheri et al., 2011; etc), the software is strong and frequently used in hydraulic simulations (Brethour and Burnham, 2010). One of the unique features of the simulator is its extremely appropriate graphic results, as it is capable of displaying the dynamic and animated behavior of fluids in 2D and 3D.

Although 2D modeling usually provides further information and details of flow behavior in different points as compared to a 1D model, it never means that the 2D modeling results are more accurate. On the other hand, fluctuations and non-convergence are seen less in 1D results (Mahjoob ~~et al., 2012~~ and Ghiassi, 2011). (The 1D data are the same direct sampling from the wetland). Therefore, this research used the results for the relationship between points and elimination of fluctuations and non-convergence. In this research, a 1D model was prepared using HEC-RAS and its results were used in text format as the input data for the 2D model. If necessary, the results of the 2D model were corrected.

RESULTS

Table 1 shows the mean field-measured values (NO_3-N) and (PO_4^{-3}) in spring, summer, autumn, and winter in 2018-2019.

Table 1: The mean field-measured values of nitrate and phosphate in spring, summer, autumn, and winter in 2018-2019.

	Spring		Summer		Fall		Winter		Average Seasons	
No. Station	**NO_3-N (mg/l)**	**PO_4^{-3} (mg/l)**	**NO_3-N (mg/l)**	**PO_4^{-3} (mg/l)**	**NO_3-N (mg/l)**	**PO_4^{-3} (mg/l)**	**NO_3-N (mg/l)**	**PO_4^{-3} (mg/l)**	**NO_3-N (mg/l)**	**PO_4^{-3} (mg/l)**
	Mean ± SD	Mean ± SD	Mean ± SD	Mean ± SD	Mean ± SD	Mean ± SD	Mean ± SD	Mean ± SD	Average	**Average**
1	2.31 ± 0.077	0.049 ± 0.061	1.95 ± 0.064	0.035 ± 0.080	1.40 ± 0.098	0.31 ± 0.034	0.77 ± 0.023	0.498 ± 0.011	1.607	**0.223**
2	2.07 ± 0.070	0.121 ± 0.026	1.88 ± 0.068	0.033 ± 0.087	1.34 ± 0.034	0.47 ± 0.056	0.73 ± 0.042	0.484 ± 0.033	1.505	**0.273**
3	2.48 ± 0.052	0.052 ± 0.090	2.35 ± 0.055	0.045 ± 0.024	1.39 ±0.06	0.48 ± 0.028	0.77 ± 0.042	0.564 ± 0.011	1.747	**0.285**
4	2.27 ± 0.049	0.063 ± 0.023	2.26 ± 0.051	0.052 ± 0.071	1.42 ± 0.051	0.40 ± 0.087	0.72 ± 0.049	0.716 ± 0.031	1.667	**0.307**
5	1.95 ± 0.086	0.148 ± 0.099	2.38 ± 0.079	0.052 ± 0.053	1.72 ±0.093	0.47 ± 0.026	0.70 ± 0.076	0.550 ± 0.028	1.687	**0.305**
6	1.69 ± 0.059	0.055 ± 0.066	2.06 ± 0.068	0.043 ± 0.075	1.74 ±0.052	0.53 ± 0.039	0.68 ± 0.066	0.649 ± 0.082	1.547	**0.319**
7	1.73 ± 0.063	0.049 ± 0.029	1.89 ± 0.067	0.319 ± 0.089	1.55 ± 0.038	0.55 ± 0.033	0.66 ± 0.063	0.575 ± 0.006	0.985	**0.373**
8	2.31 ± 0.071	0.072 ± 0.078	2.33 ± 0.066	0.132 ± 0.091	1.27 ±0.035	0.50 ± 0.027	0.73 ± 0.028	0.602 ± 0.019	1.660	**0.326**
9	1.75 ± 0.079	0.124 ± 0.058	2.36 ± 0.082	0.045 ± 0.035	1.42 ± 0.091	0.53 ± 0.099	0.90 ± 0.089	0.739 ± 0.035	1.607	**0.359**
10	1.80 ± 0.069	0.048 ± 0.068	2.38 ± 0.072	0.660 ± 0.028	1.63 ± 0.050	0.48 ± 0.089	0.89 ± 0.099	0.720 ± 0.032	1.675	**0.477**
11	1.68 ± 0.037	0.056 ± 0.062	2.19 ± 0.041	0.047 ± 0.061	1.43 ± 0.089	0.68 ± 0.041	0.78 ± 0.073	0.727 ± 0.061	1.520	**0.377**
12	1.87 ± 0.080	0.049 ± 0.056	1.97 ± 0.078	0.358 ± 0.026	1.57 ±0.053	0.36 ± 0.088	0.85 ± 0.061	0.570 ± 0.026	1.565	**0.334**
13	1.61 ± 0.042	0.150 ±0.083	2.39 ± 0.039	0.040 ± 0.090	1.39 ±0.046	0.33 ± 0.048	0.75 ± 0.055	0.550 ± 0.090	1.535	**0.267**
14	1.29 ± 0.059	0.049 ±0.064	2.34 ± 0.065	0.043 ± 0.023	1.50 ± 0.051	0.55 ± 0.040	0.51 ± 0.065	0.708 ± 0.023	1.410	**0.337**
15	1.28 ± 0.086	0.191 ± 0.035	2.27 ± 0.079	0.047 ± 0.099	1.76 ±0.093	0.43 ± 0.039	0.76 ± 0.068	0.616 ± 0.099	1.517	**0.321**
16	1.09 ± 0.039	0.051 ±0.072	2.21 ± 0.044	0.055 ± 0.066	1.24 ± 0.078	0.61 ± 0.039	0.89 ± 0.093	0.501 ± 0.066	1.357	**0.304**
17	0.98 ± 0.073	0.061 ± 0.051	1.95 ± 0.069	0.098 ± 0.029	1.38 ±0.038	0.68 ± 0.037	0.90 ± 0.034	0.110 ± 0.029	1.302	**0.237**
18	1.29 ± 0.071	0.147 ± 0.022	2.41 ± 0.077	0.221 ± 0.078	0.81 ± 0.035	0.46 ± 0.061	0.91 ± 0.017	0.572 ± 0.078	1.355	**0.350**
19	1.75 ± 0.079	0.146 ± 0.057	2.35 ± 0.079	0.024 ± 0.058	1.42 ± 0.093	0.54 ± 0.049	0.75 ± 0.019	0.550 ± 0.058	1.567	**0.315**
20	1.54 ± 0.059	0.058 ± 0.071	1.79 ± 0.061	0.031 ± 0.068	1.33 ± 0.005	0.47 ± 0.066	0.72 ± 0.020	0.505 ± 0.068	1.345	**0.266**
Average	1.737 ± 0.087	0.146 ± 0.080	2.20 ± 0.029	0.134 ± 0.064	1.457 ± 0.05	0.492 ± 0.07	0.785 ± 0.02	0.594 ± 0.017	**1.545**	**0.341**
Guide level	0.05* - 0.05**	0.01*	0.05* - 0.05**	0.01*	0.05* - 0.05**	0.01*	0.05* - 0.05**	0.01*	0.05**	**0.01***
Max	0.1* - 0.5**	0.1*	0.1* - 0.5**	0.1*	0.1* - 0.5**	0.1*	0.1* - 0.5**	0.1*	0.5**	**0.1***

* –OECD (1982)
** –80/778/EEC

Selection of the Best Interpolation Method

To select the best RMSE, a series of calculations were made to choose the best power and order for some of the interpolation and extrapolation methods used in this research. RMSE results showed that power 1 (among powers 1-6) is the best power (with minimum RMSE value) for interpolation operation using inverse distance to power 2 (among powers 2, 5, and 10) and order 1 (among orders 1, 2, and 3) is the best order for local polynomial method. (It should be noted that this power was achieved using inverse validation method.)

Table 2 shows the calculated RMSE values in brief. The values in the table include the minimum RMSE of each method achieved by optimizing the parameters of each method. Based on the inverse validation method, comparison of interpolation results (Table 2) shows that the best method to estimate nitrate and phosphate concentration values in Anzali Wetland is order 2 polynomial regression method (with the mean RMSE = 0.2075 for nitrate and RMSE = 0.1475 for phosphate). After that, inverse distance to power 2 method can be a suitable option. Compared to other methods, the most inappropriate results are related to the local polynomial method (with the mean RMSE=0.331 for nitrate and RMSE=0.22 for phosphate).

Model Calibration and Verification

Model parameters were calibrated and adjusted with respect to the available data and simulated data systematically. Model parameters were changed by trial and error method and using local measured data, parameters, and assumptions in a way that the results obtained from modeling gained further compatibility

Table 2: Comparison of RMSE values of different interpolation methods for nitrate and phosphate in 2018-2019.

Amount / Methods	RMSE (Winter)		RMSE (Fall)		RMSE (Summer)		RMSE (Spring)	
	PO_4^{-3}	NO_3-N	PO_4^{-3}	NO_3-N	PO_4^{-3}	NO_3-N	PO_4^{-3}	**NO_3-N**
Kriging	0.25 (0rder 1)	0.19 (0rder 1)	0.19 (0rder 2)	0.24 (0rder 1)	0.32 (0rder 1)	0.39 (0rder 1)	0.06 (0rder 1)	**0.45 (0rder 2)**
Inverse distance to power	0.22	0.17	0.19	0.21	0.34	0.34	0.06	**0.44**
Polynomial Regression	0.17 (Power of 3)	0.11 (Power of 2)	0.14 (Power of 2)	0.15 (Power of 1)	0.24 (Power of 2)	0.25 (Power of 2)	0.04 (Power of 1)	**0.32 (Power of 2)**
S-plus	0.28	0.18	0.20	0.24	0.33	0.39	0.06	**0.48**
Local polynomial	0.25	0.20	0.22	0.23	0.35	0.40	0.06	**0.49**

compared to the ones obtained from local measurements. To do so, the model was implemented about 20 to 50 times using trial and error to achieve the results of an acceptable calibration. Curves 6 and 8 clearly show the accuracy and precision of the functions. As nitrification and denitrification processes and temperature are effective in nitrate simulation, the coefficients of the processes were calibrated by the model. In addition, modeling accuracy was calculated by HEC-RAS and the parameters such as correlation coefficient (R^2) and mean absolute error (MAE) were calculated by Equation (37) which its results are shown in tables 3 and 4. Simulation calibration was performed at the end of each period with respect to the existing data and simulated factors. Figures 5 to 8 show calibration and verification curves.

$$MAE = \frac{1}{N}\sum_{i=1}^{N}(X_P - X_0)_i \tag{37}$$

where X_0 and X_p are respectively the observed (measured) values and the simulated values and N is the number of specimens (Shokri et al., 2018).

Table 3: Model accuracy examination at calibration stage.

Parameter / Index	NO_3-N	PO_4^{-3}
R^2	0.9137	**0.9214**
MAE	0.090	**0.038**

Table 4: Model accuracy examination at verification stage.

Parameter / Index	NO_3-N	PO_4^{-3}
R^2	0.950	**0.910**
MAE	0.008	**0.090**

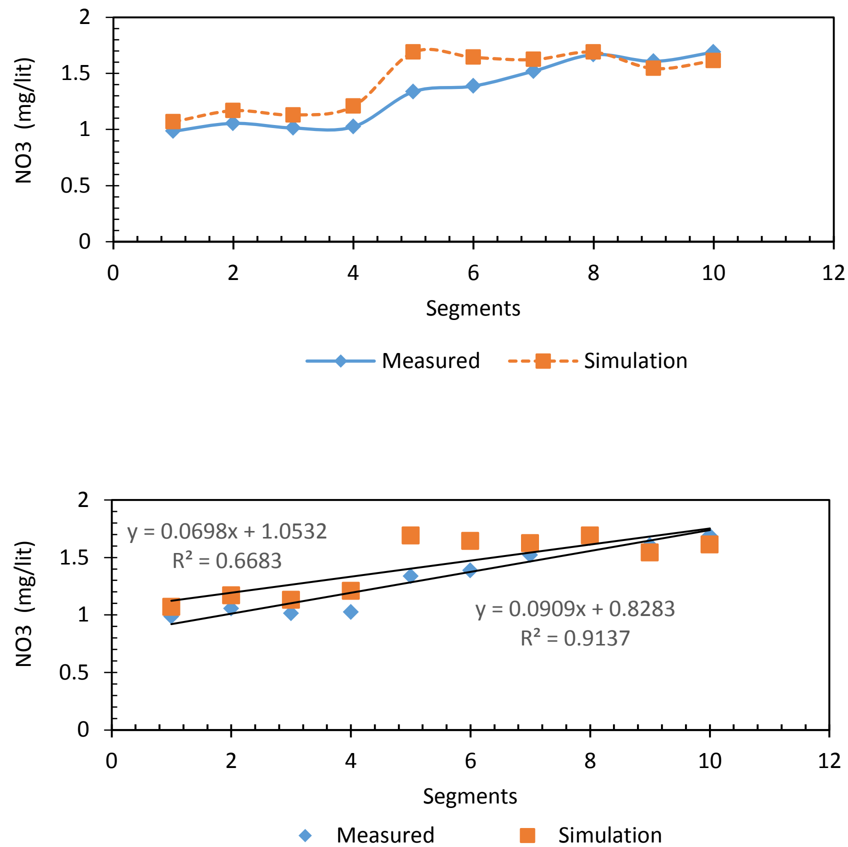

Figure 5. Changes in mean nitrate levels and correlation rate at the model calibration stage at different points across the wetland.

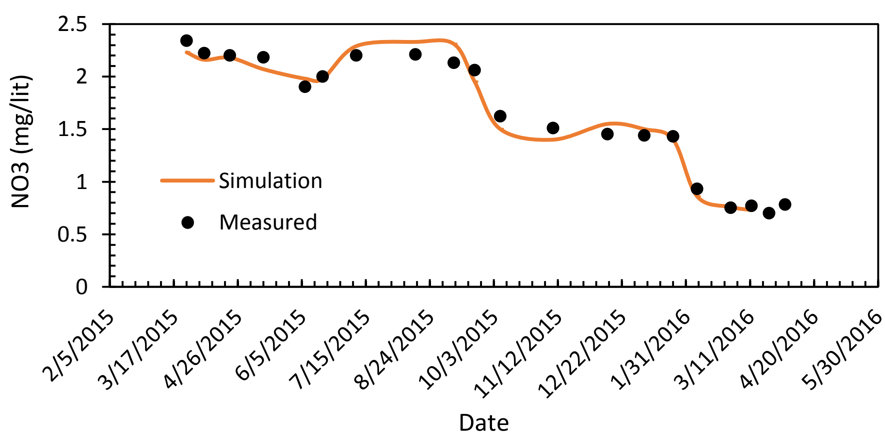

Figure 6. Curve of changes in mean nitrate levels at the model verification stage at different points across the wetland.

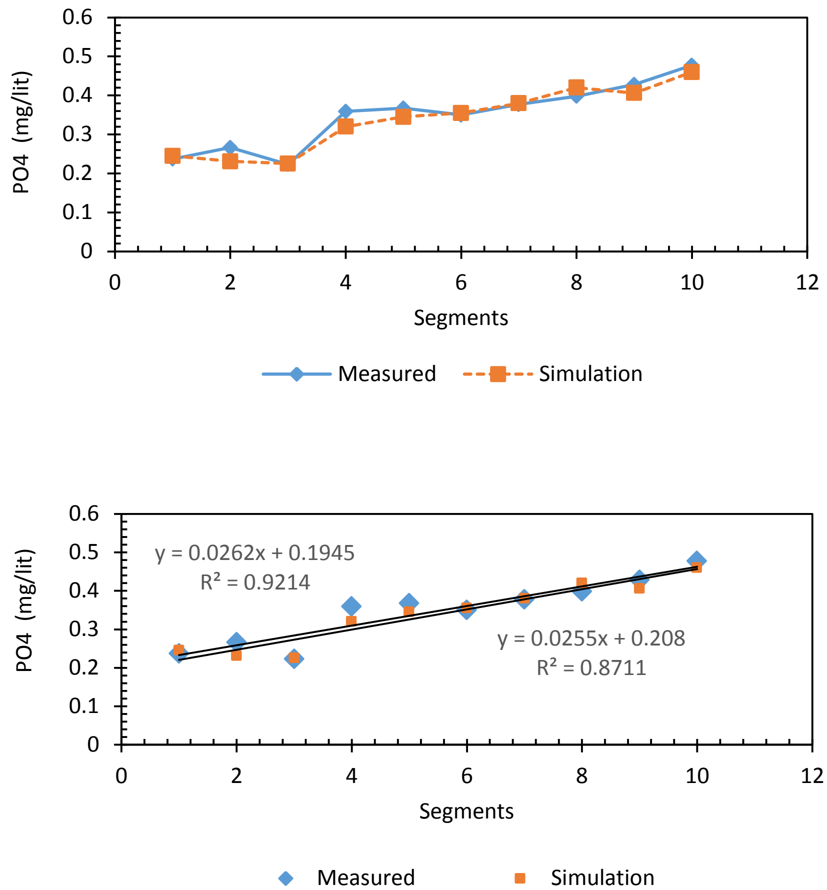

Figure 7. Changes in mean phosphate levels and correlation rate at the model calibration stage at different points across the wetland

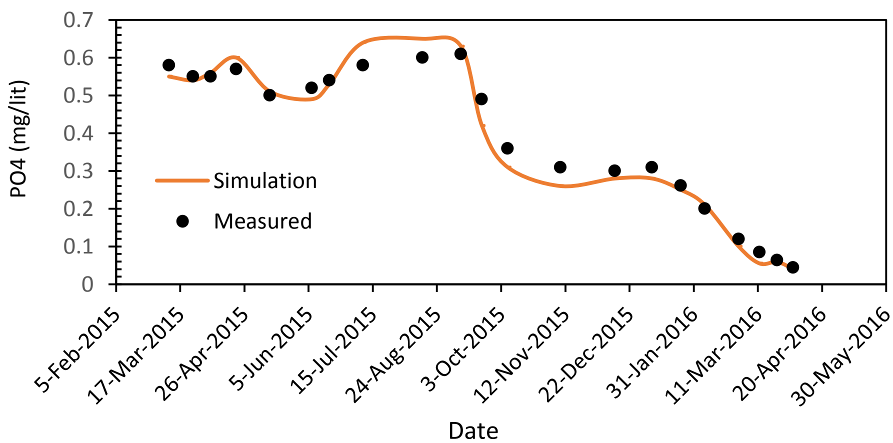

Figure 8. Curve of changes in mean phosphate levels at the model verification stage at different points across the wetland

2D Flow Analysis Correction using 1D Accurate Contents

As the changes of hydraulic parameters such as the changes of velocity and the change of velocity and water flow direction in the study are are effective in material distribution in water, necessary studies were carried out on the shallow waterbed (wetland) to examine the correct function of the model. For this purpose, the model results were compared to the results of the studies conducted by Yang et al.(2005). In all models, the input boundary condition in the flow upstream (wetland inlet) was considered the fixed flow and velocity gradient and depth gradient were considered zero in the flow upstream (wetland outfall). The results of SKE model, Spezial model, and laboratory model were presented using the studies of Yang et al.(2005). The geometry field of the wetland bed was defined in figure 4 to show the analysis and calibration results of the model. Number of the elements on axes *X* and *Y* are 60 and 25 elements, respectively.

The 1D model was prepared by HEC-RAS (the flow 1D data are the same accurate data obtained from the direct sampling of the wetland) and the results were used in *text* format as the input data for the 2D model. Figure 9 shows that the flow relative velocity in longitudinal and latitudinal cross-sections of the waterway is of the results of SKE, Spezial, and laboratory models in this research. The Uref parameter of flow velocity is in the wetland inlet prior to estuaries. Figure 9 shows an appropriate agreement among the model results, the numerical studies, and the laboratory model of Yang et al.(2005), which confirms software performance. The only fluctuation control method in the 2D flow model is to adjust the 2D model using the 1D model results. Lack of fluctuation in the results indicates the success of fluctuation control using the presented idea. The use of 1D results accelerated convergence solution in the 2D model and reduced the size and volume of calculations to achieve the final answer.

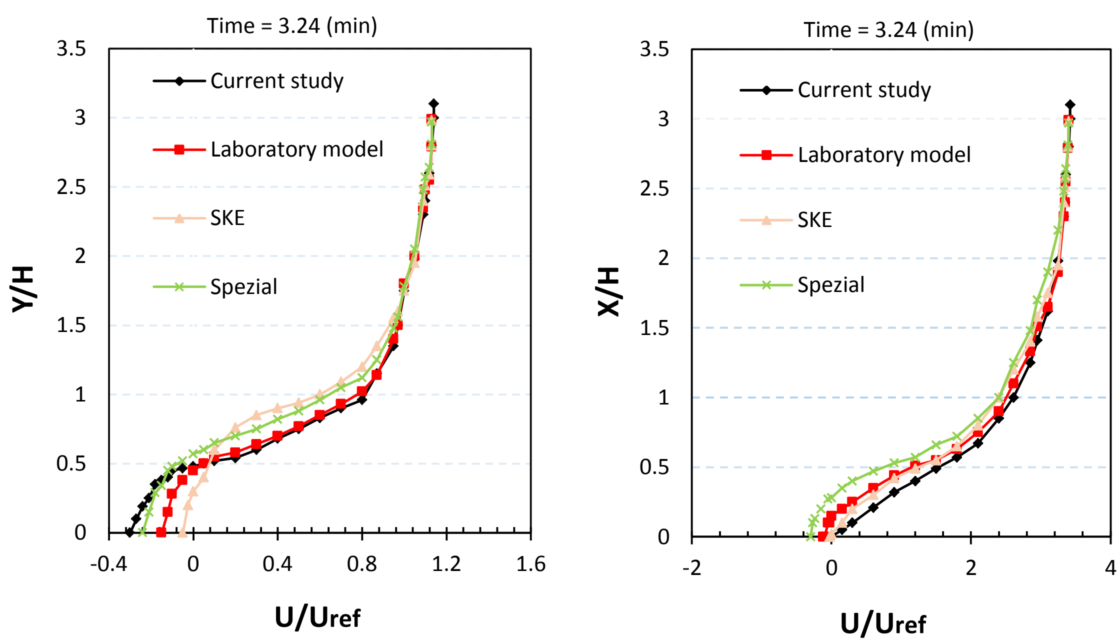

Figure 9. Diagram of flow relative velocity in the longitudinal and transverse -sections of the waterway bed.

Drawing the calculated flow lines in figure 10 is among other presentable results of the modeling in shallow water.

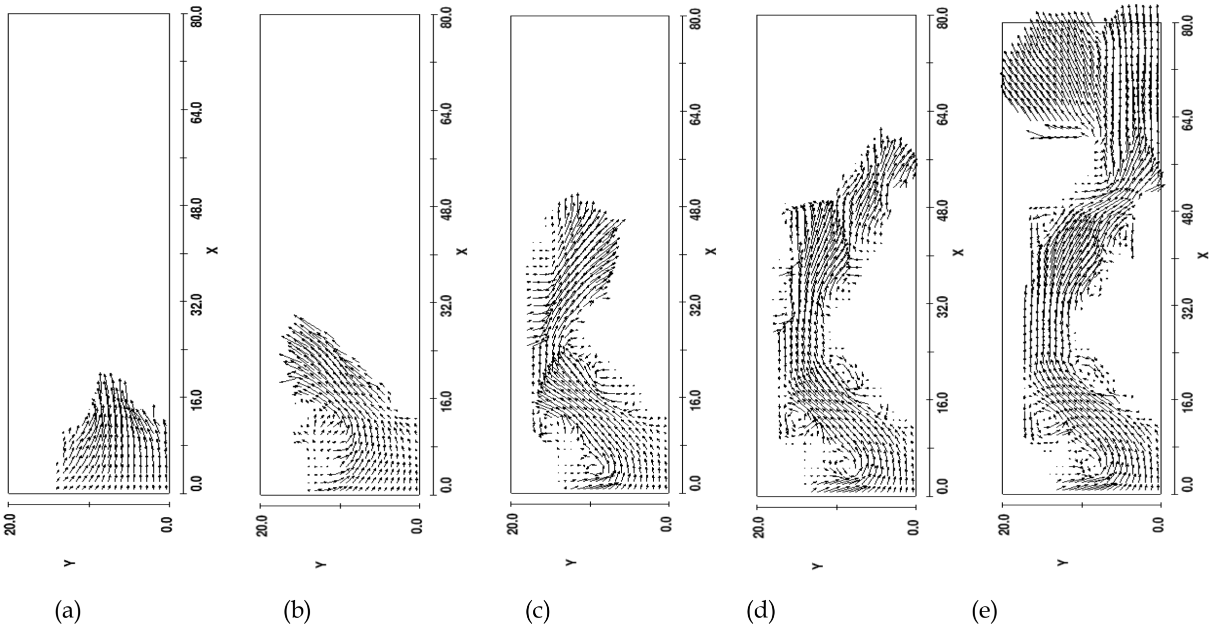

Figure 10. Flow lines and profiles of velocity vectors in the wetland using the model in the calculation network of x/h=40 and y/h=10 in minutes 0.32 (a), 0.97 (b), 1.61 (c), 2.49 (d), and 3.24 (e).

Examination of Zoning Maps

Since the study of seasonal changes of surface water quality is a major aspect in examining temporal changes of wetlands pollution (Ouyang et al., 2006), the distribution of changes in phosphate and nitrate concentration in different seasons was determined. Seasonal maps were prepared after extracting the monthly concentration map for phosphate and nitrate using order 2 polynomial regression method. Figures 11 and 12 show the spatial seasonal distribution maps for nitrate and phosphate extracted from Anzali Wetland in MATLAB. Comparison of figure 10 and Figures 11 and 12 shows that nitrogen and phosphorus concentration is very high in the places with low velocity and water flow, especially at edges and in reedy regions, and the minimum concentration of nutrients is seen where vortices are formed.

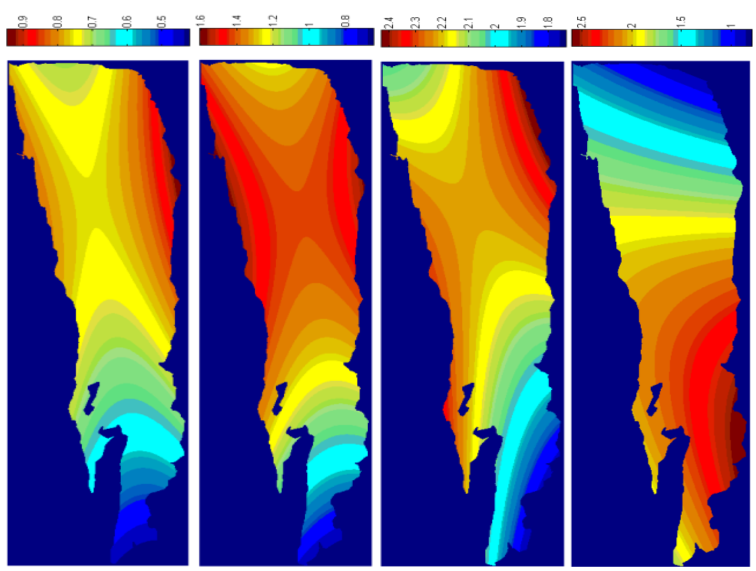

Figure 11. Seasonal plans spatial distribution of nitrate (mg/L) in Anzali Wetland in spring (a), summer (b), autumn (c), and winter (d) in 2018-2019.

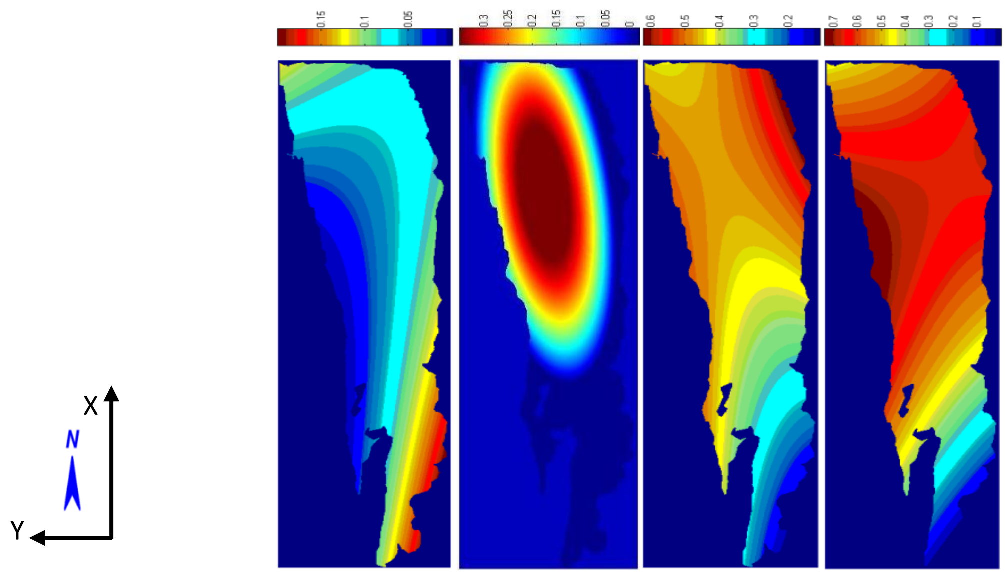

Figure 12. Seasonal plans spatial distribution of phosphate (mg/L) in Anzali Wetland in spring (a), summer (b), autumn (c), and winter (d) in 2018-2019

DISCUSSIONS

The considerable increase in the nitrate concentration average (1.545 mg/l) and phosphate (0.341 mg/l) over the past two decades and its comparison with the previous similar studies in other wetlands and water resources (Mirbagheri et al. 2011; Aliverdi and Eslami 2014; Salmani 2016) can be considered as one of the major indices for eutrophication of the aqueous environment. It can be concluded that the study basin ,which is subject to the advanced eutrophication conditions (OECD, 1982), has considered oligotrophic conditions for the nitrate content below 0.1 mg/l, mesotrophic conditions for the nitrate content between 0.1-0.2 mg/l, and eutrophic conditions for the nitrate content above 0.2 mg/l).

According to the international standards, the usual phosphorus content between 0.1 and 0.2 mg/l is sufficient to accelerate eutrophication (Naseri and Ghaneian, 2004; 80/778/EEC). Although the increase of nutrients in aqueous ecosystems is natural and they increase gradually in their lifetime, such phenomena require tens of centuries or longer period to occur (Seng Lung, 2001).

The average nitrate content in Anzali Wetland in summer and spring exceeds autumn and winter (Figure 6); however, the average content of phosphate in winter and autumn exceeds spring and summer (Figure 8). The amount of nitrate and phosphate is low; however, its contents increase along the route due to the estuaries of wetland bed, reduction of water flow velocity, further flow of pollutants produced in fish ponds, and the increase in suspended sediments flowing into the wetland. Since no a specific source of pollution after the Anzali Wetland Bridge was included in the model, the model considered a fixed content of nitrate. As figure 11 shows, nitrate and phosphate concentration in the eastern and southeastern part of the wetland exceeds the western part because the major incoming water flows and excess water of rice field under irrigation are located in the eastern part of the wetland.

Comparison of spatial change maps of phosphate and nitrate concentration in different seasons (figures 5, 7, 11, and 12) shows a positive 6-7% correlation between nitrate and phosphate concentrations. When phosphate concentration in a section of the wetland is high, nitrate concentration in the same section is high, too. When phosphate concentration in a section of the wetland is low, nitrate concentration in the same section is also low.

An increase and decrease process similar to the one of nitrate and phosphate in the wetland may imply that phosphate and nitrate have probably common pollution resources. Of course, factors such as land use pattern, management practices, soil properties and geomorphology have an impact on phosphate (and nitrate) levels (Boluwade and Madramootoo, 2013).

Average relative reduction of DO in water (3.58 mg/l), comparison between this study and the similar studies in other water resources (Bhor et al., 2013; Salmani, 2016; Al-Badaii et al., 2014), the overgrowth of aquatic plants, especially Azola, abundance of planktonic biomass in the basin emphasize that the study area is being exposed to critical eutrophication. DO content is relatively high (3.95 mg/l); however, it reduced to 2.84 mg/l along the route due to the closure of wetland bed, the flow of agricultural non-point pollutants resources, and urban wastewater drainage (point resources).

CONCLUSION

The results showed that it was possible to prepare and predict the zoning map for the seasons and changes of spatio-temporal distribution of water quality parameters including nitrate, phosphate, and dissolved oxygen in different water basins using 2D equations of shallow water and their numerical solution and the technique to use the best interpolation method. Based on the research, the velocity and direction of the hydraulic flow of water can be determined and their impacts on water quality parameters can be studied. The idea of using the 2D flow correction analysis in wetlands using 1D accurate values is another major results of the research that leads to fluctuation reduction in results and achieves better convergence in solving the obtained equations, as it reduced the time and volume of calculations to reach the final answer.

Based on the research, the mean nitrate and phosphate concentration of in the basin (Anzali Wetland) is higher than the permissible amount, according to the European Instruction 80/778/EEC and OECD standards, which shows that the area has a weak self-purification capability. It can confidently be mentioned that the basin is subject to advanced eutrophication conditions. The results obtained from simulating the numerical model and the author-developed software prove that the average annual concentration of nitrate and phosphate in the basin in 2020 will respectively be about (3.7%) and (6.2%) higher than the present values and the average relative DO will reduce about (5.8%). In 2030, the values will be about (10.1%), (15.5%), and (14.7%), respectively. The comparison between the results calculated by the simulator and laboratory-measured values shows that there is an appropriate agreement between the model and real conditions.

Acknowledgments

The authors thank the esteemed authorities of Bandar Anzali Synoptic Meteorological Station and Environmental Protection Organization of Gilan Province, especially Azam Al-Sadat Mir Roshandel (PhD) and Babak Kakavandi (PhD) for their kind cooperation and assistance in the project steps.

ADDITIONAL INFORMATION AND DECLARATIONS

Funding

There was no funder for this study.

Grant Disclosures

There was no grant funder for this study.

Competing Interests

The authors declare there are no competing interests.

Author Contributions

Homami Majid conceived the experiments, analyzed the data, prepared figures, and tables, authored or revised drafts of the paper, approved the final draft.

To conduct the research, the required data such as geometrical and waterway topography data, hydraulic data, meteorological data for 2018-2019 were obtained from *Bandar Anzali Synoptic Station* (Meteorological Organization 2000-2012) and the sampled data were provided from *Environmental Protection Agency (EPA) of Gilan Province*. The required kinetic coefficients were applied to model equations and boundary conditions were applied to the software.

Data Availability

All the data are shown in the tables of this article.

Ethics Statement

The study was approved by Scientific Association of Environmental Education and Sustainable Development(EESD) http://www.ac.ir/environment and College of Environment.

Supplemental Information

Supplemental information for this article can be found online at http://esa.uoe.ir/

REFERENCES

Al-Badaii, F., Othman, M. S. & Gasim, M. B. (2013). Water quality assessment of the semenyih river, selangor, Malaysia., Journal of Chemical, 1-9. http://dx.doi.org/10.1155/2013/871056

Aliverdi, A. R. & Eslami, H. (2014). Modeling quality parameters nitrate and ammonia in the river between the bridge Elhayi using software WASP6. The first national conference on architecture, civil engineering and urban environment, Hamedan, Community environmental assessment hegmataneh. Available from http://www.civilica.com/Paper-ARCHITECTURE01-ARCHITECTURE01_437.html

Bhro, M., Kadave, P., Bhor, A., Bhro, S., Bhosale, M. & Bholay, A. D. (2013). Water quality assessment of the river godavari, at Ramkund, Nashik, (Maharashtra), India. International Journal Engineering Science, 2(2), 64-68.

Biglarijoo, N., Mirbagheri, S. A., Bagheri, M. & Ehteshami, M. (2017). Assessment of effective parameters in landfill leachate treatment and optimization of the process using neural network, genetic algorithm and response surface methodology. Process Safety and Environmental Protection, 106, 89-103.

Boluwade, A. & Madramootoo C. A. (2013). Assessment of uncertainty in soil test phosphorus using kriging techniques and sequential Gaussian simulation: implications for water quality management in southern Quebec. Water Quality Research Journal Nov 2013, 48 (4) 344-357.

Bottino, F., Ferraz, I. C., Mendiondo, E. M. & Carmo Calijuri, M. (2011). Calibration of QUAL2K model in Brazilian micro watershed: effects of the land use on water quality. Acta Limnologica Brasiliensia, 22(4), 474-485.

Brethour, J. & Burnham, J. (2010). Modeling sediment erosion and deposition with the FLOW-3D sedimentation & scour model.

Burton, T. M. & Tiner, R. W. (2009). Ecology of wetlands, In: Likens G.E. (ed.) Encyclopedia of Inland waters. Elsevier, Inc, Amsterdam, pp. 507–515.

Dorostkar, A. & Etemad-Shahidi, A. (2005). A Two-Dimensional laterally averaged model for lakes, reservoirs and estuaries. Sixth International Conference on Coasts, Ports and Offshore, Ports & Shipping, Tehran, Iran. http://www.civilica.com/Paper-ICOPMAS06-ICOPMAS06_019.html

European Directive 80/778/EEC. Human consumption water quality.

Forsythe, K. W., Paudel, K. & Marvin, C. H. (2010). Geospatial analysis of zinc contamination in lake Ontario Sediments. Environmental Informatics 16(1), 1-10.

Haji, A. H., Mirbagheri, S. A. & Javid, A. H. (2013). A wavelet support vector machine combination model for daily suspended sediment forecasting. International Journal of Engineering Transfer (IEJ), 27(6), 855.

Hasani Pak, A. A. (2013). Geostatistical. Tehran University Published, p. 76.

JICA (Japan International Cooperation Agency), (2012). Zoning plan in the Anzali wetland, Anzali wetland ecological management project in Islamic Republic of Iran. Report number: 2, p. 95.

Johnston, K., VerHoef, J. M., Krivoruchko, K. & Lccas, N. (2001). Using ArcGIS Geostatistical Analyst. New Yourk, USA.

Jones, K. 2008 Monitoring and assessment of wetlands using Earth Observation. Journal of Environmental Management. Article in press.

Kazemi, S. M. & Hosseini, S. M. (2011). Comparison of spatial interpolation methods for estimating heavy metals in sediments of Caspian Sea. Expert Systems with Applications 38, 1632–1649.

Mahjoob, A. & Ghiassi, R. (2011). Application of a coupling algorithm for the simulation of flow and pollution in open channels. World Application Scientific Journal, 12(4), 446-459.

Majnonian, H. (2003). Classified and protected wetlands, value and functions. Department of the Environment Iran, p. 24.

Meteorological Organization, (2012). Synoptic station of Anzali port, the obtained data of 2000-2012.

Miller, J. J., Bremer, E., Curtis, T. & Chanasyk, D. S. (2017). An assessment of nutrient dynamics in streambank soils of the lower little bow river in southern Alberta using ion exchange membranes. Water Quality Research Journal, Available Online 3 July 2017, wqrjc2017007; DOI: 10.2166/wqrj.2017.007

Mirbagheri, S. A. & Tanji, K. K. (1981). Sediment characterization and transport modeling in Colusa Drain, California. University of California at Davis. Department of Land, Air, and Water Resources.

Mirbagheri, S. A., Tanji, K. K. & Krone, R. B. (1988). Simulation of suspended sediment in Colusa Basin Drain, California. Journal Environment, ENG-ASCE, 114(6), 1275-1294.

Mirbagheri, S. A. & Hashemi, S. A. H. (2008). Nutrient transport model in Chah nimeh manmade reservoir. Proceedings of the 8th conference on systems theory and scientific.

Mirbagheri, S. A., Nouri, J., Farokhian, F. & Jafarzadeh, N. (2010). Water quality variability and eutrophic state in wet and dry years in wetlands of the semiarid and arid regions. Environment Earth Science, 59(7), 1397-1407.

Mirbagheri, S. A., Mahmodi, S. & Khezri, S. M. (2011). Simulation modeling of nitrogen and phosphorous change in Chalous river. Journal Civil Environment Engineering (University of Tabriz), 40(3), 47-59 (In Persian).

Mirbagheri, S. A., Sadrnejad, S. A. & Hashemi, M. S. A. (2012). Phytoplankton and zooplankton modeling of Pishin Reservoir by means of an advection-diffusion drought model. International Journal Environment Resource (IJER), 6(1), 2012.

Mirbagheri, S. A., Ahmadi, S. & Biglari-Joo, N. (2016a). Denitrification of nitrate-contaminated groundwater in an anoxic rotating biological contactor: a case study. Desalination and Water Treatment 57 (10), 4694-4700.

Mirbagheri, S. A., Avili, F. G. & Javid, A. H. (2016b). Modeling arsenic transport in soil column and ground water. BULGARIAN CHEMICAL COMMUNICATIONS 48, 199-204.

Mitsch, W. J. & Gosselink, J. G. (2007). Wetlands. John Wiley & Sons, Inc, NewYork, pp. 582.

Mohamadi Golafshani, N., Mosavi, A. & Bostani, F. (2012). Pollution of river water quality management using simulated by mathematical models wasp (Case Study: Talar rivers). The first national conference on environmental protection and planning, Hamedan, Islamic Azad University, Hamedan. Available from http://www.civilica.com/Paper-NATURE01-NATURE01_812.html

Mohamadzadeh, G. M. & Namin M. M. (2005). Simulation of free surface flows by Projection Method. Iranian Hydraulic Conference, Shahid Bahonar Kerman University, Kerman, Iran.

Muhammetoglu, A. & Soyupak, S. (2000). A three-dimensional water quality-macrophyte interaction model for shallow lakes. Ecology Modell. 133, 161-180.

Naseri, S. & Ghaneian, M. T. (2004). Quality management lakes and tributary rivers. Nas Publishers, One Edition.

OECD, Vollenweider, R. A. & Kerekes, J. (1982). Eutrophication of waters. Monitoring, assessment and control. OECD Cooperative programme on monitoring of inland waters (Eutrophication control), Environment Directorate, Paris, p. 154.

Ouyang, Y., Nkedi-Kizza, P., Wu, Q. T., Shinde, D. & Huang, C. H. (2006). Assessment of seasonal variations in surface water quality. Water Resource, 40(20), 3800-3810 (In Persian).

Sabbagh-Yazdi, S. R., Mastorakis, N. E. & Hosseini-Gelekolai, S. M. (2008). Comparing central and upwind flux averaging schemes of overlapping finite volume method for simulation of spillway flow with shock waves, International Journal of Computers, 2 (1), 23-31.

Salmani, M. H. & Salmani Jajaei, E. (2016). Forecasting models for flow and total dissolved solids in Karoun river-Iran. Hydrology 535, 148–159.

Seng Lung, W. (2001). Water quality modeling for waste lode allocations and TMDLS. Published simultaneously in Canada.

Shoaei, S. M., Mirbagheri, S. A. & Zamani, A. (2018). Seasonal variation of dissolved heavy metals in the reservoir of Shahid Rajaee Dam, Sari, Iran. Desalination and Water Treatment, 56(12), 3368-3379.

Shokri, S., Hoshmand, E. A. & Moazed , H. (2015). Investigation of chemical water quality Gargar river by graphical methods and multivariate statistical analysis. Journal of Lagoon ecobiology, 3(20), 19-33 (In Persian).

Viera, S. R., Rielson, D. R. & Biggar, J.W. (1983). Geostatistical theory and application to variability of some agronormical properties. Hilgardia 51(3), 1–75.

Yang, X. D., Ma, H. Y. & Huang, Y. N. (2005). Prediction of homogeneous shear flow and a backward-facing step flow some linear and non-linear K-e turbulence models. Communications in Nonlinear Science and numerical Simulation 10, 315-328.

Zarrati, A. R., Tamai, N., Islam, G. M. T. & Huang, G. (2001). Prediction of water surface elevation in a channel with continuous bends. Proceedings of 29th IAHR Congress, Beijing, China, 95-104.

Zebardast, L. & Jafari, H. R. (2012). Evaluation process changes in Anzali wetland using remote sensing and providing management solution. Journal of Environmental Studies, Vol. 37, No. 57, pp. 57-64.